mathematics

Article

Design of Linear Matrix Inequality-Based Adaptive Barrier Global Sliding Mode Fault Tolerant Control for Uncertain Systems with Faulty Actuators

Kamran Naseri [1,†], Mai The Vu [2,†], Saleh Mobayen [1,3,*], Amin Najafi [1] and Afef Fekih [4]

1 Department of Electrical Engineering, University of Zanjan, Zanjan 45195-313, Iran; ing.naseri@gmail.com (K.N.); aminnajafi@znu.ac.ir (A.N.)
2 School of Intelligent Mechatronics Engineering, Sejong University, Seoul 05006, Korea; maithevu90@sejong.ac.kr
3 Future Technology Research Center, National Yunlin University of Science and Technology, Douliou 64002, Yunlin, Taiwan
4 Department of Electrical and Computer Engineering, University of Louisiana at Lafayette, Lafayette, LA 70504, USA; afef.fekih@louisiana.edu
* Correspondence: mobayens@yuntech.edu.tw
† Kamran Naseri and Mai The Vu are the first authors; these authors contributed equally to this work.

check for updates

Citation: Naseri, K.; Vu, M.T.; Mobayen, S.; Najafi, A.; Fekih, A. Design of Linear Matrix Inequality-Based Adaptive Barrier Global Sliding Mode Fault Tolerant Control for Uncertain Systems with Faulty Actuators. *Mathematics* **2022**, *10*, 2159. https://doi.org/10.3390/math10132159

Academic Editor: Asier Ibeas

Received: 20 May 2022
Accepted: 19 June 2022
Published: 21 June 2022

Abstract: This paper proposes a linear matrix inequality (LMI)-based adaptive barrier global sliding mode control (ABGSMC) for uncertain systems with faulty actuators. The proposed approach is derived using a novel global nonlinear sliding surface to guarantee the global dynamic property and to ensure system stability and the occurrence of sliding in the presence of actuator faults. The optimal coefficients of the sliding surface are determined using the LMI method. The system's asymptotic stability is proven using Lyapunov theory. Additionally, an adaptive barrier function is considered to ensure the convergence of the output variables to a predefined locality of zero in a limited time, even where external disturbances and actuator faults are present. In order to decrease the steepness of the control action and mitigate the chattering phenomenon, the hyperbolic tangent function is employed instead of the signum function in the sliding mode control. The proposed method is validated using a simulation study of the Genesio's chaotic system.

Keywords: sliding mode control; actuator fault; linear matrix inequality; adaptive control; uncertain system

MSC: 93C40; 93D21; 94C12; 68M15; 62F35; 93D09; 93C10

1. Introduction

Modern technological systems are complex and highly interconnected. They are also vulnerable to faults, as a fault in a single element can easily propagate throughout the whole system. Actuator faults can drastically decrease the performance of control systems and potentially lead to total failures and costly shutdowns. External disturbances, parametric uncertainties resulting from wear and tear, and changing operating conditions also reduce the efficiency and reliability of dynamic systems and can lead to system instability. Hence, much effort has been made in recent decades to develop systems with fault-tolerant capabilities so as to ensure system safety, reliability, and availability [1,2]. Faults are defined as the impermissible deviation of the system structure or the system parameters from the nominal situation [3–5]. Faults are often classified as plant faults, sensor faults, and actuator faults. Faults can also be distinguished based on their size and temporal behavior as abrupt faults (step-wise), incipient faults (drift-like), and intermittent faults. Fault-tolerant controls (FTCs) are control systems designed to maintain satisfactory system performance under faulty conditions [6]. FTCs are typically classified as an active FTC (AFTC) and a passive

FTC (PFTC). AFTC approaches rely on a fault detection and identification (FDI) unit to explicitly detect and estimate faults, whereas PFTC approaches are designed to be robust against certain faults without the need for explicit detection [7,8]. The latter are more conservative than the AFTC, but they are less computationally expensive.

Several control techniques have been considered in the literature to design PFTC approaches. For instance, Ref. [9] considered an LMI scheme, an H_∞ approach was adopted in [10], a sliding mode control (SMC) approach was adopted in [11,12], and an adaptive SMC (ASMC) was adopted in [13–16]. Fuzzy logic [17,18], neural networks (NN) [19,20], and model predictive control (MPC) [21,22] have also been considered. Among the above-listed approaches, the SMC technique has drawn much attention due to its ability to eliminate parametric uncertainties and mitigate the effects of external disturbances and faults [23–28]. SMC is achieved using two main phases: the sliding phase and the reaching phase. A sliding surface is defined so as to obtain the desired dynamics of the controlled system in the sliding mode. Once the states reach the sliding surface, an affiliated control law is designed to execute the sliding mode and guarantee the system's invariance to external disturbances and uncertainties. However, the invariance of SMC to uncertainties is not guaranteed in the reaching phase when linear sliding surfaces are adopted [29]. Additionally, the practical implementation of SMC with linear sliding surfaces often leads to oscillations with finite frequency and amplitude, otherwise known as the chattering phenomenon [30]. Integral terminal sliding mode controls (ITSMC) have been proposed to mitigate this problem and ensure the convergence of the states to the smallest vicinity of zero at a finite time.

An integrated FD and FTC design was proposed in [31] for a reverse osmosis desalination unit. A parity space technique was considered to approximate actuator faults, and a receding-horizon predictive control-bounded data uncertainties controller was considered to compensate for the extant uncertainty generated by the model and observer. A nonlinear robust FTC approach was proposed in [32,33] to mitigate wind perturbations and actuator faults in a quadrotor system. Actuator faults and wind disturbances were estimated using an adaptive time-extended observer. Tracking performance was ensured using a continuous FTSMC approach. A radial basis function (RBF) neural network-based FTC strategy was considered in [34] for Markovian jump systems (MJSs) subject to faults and nonlinear dynamics. The proposed control approach was based on an adaptive backstepping technique and was shown to completely mitigate for the effects of actuator faults and nonlinearities while also guaranteeing system stability. A control allocation approach based on adaptive sliding mode control (ASMC) was proposed in [35] for distributed-driven electric vehicles subject to actuator faults. A state observer (SO) was considered to obtain an estimate of the sideslip angle in the control layer, and a barrier function was adopted to enhance the robustness of the ASMC approach. The main reason for choosing the barrier function was to prevent undesirable effects via the use of cost functions. The closed-loop system's insensitivity to faults and disturbances is ensured by the sliding mode controller. The implementation of a controller requires exact knowledge about the upper bounds of disturbances and noise in order to limit the effects of chattering; however, this information is often unavailable in practical applications.

This paper proposes an adaptive barrier terminal GSMC approach based on LMI and hyperbolic tangent functions. Its main contributions are as follows:

- Using the global sliding method control based on LMI, the best and most optimal sliding coefficient is obtained.
- A design that considers a barrier function without information about the upper bound of perturbations and actuator faults, which makes the system track the desired path with the least chattering possible, is proposed.
- An SMC design that relies on the hyperbolic tangent function to further reduce chattering.

The remainder of this article is organized as follows: Section 2 provides the problem description, along with some preliminaries. Section 3 derives the proposed controller and discusses the stabilization analysis. The simulation results are detailed in Section 4. Finally, some concluding remarks are given in Section 5.

2. Problem Description and Preliminaries

Assume the following system:

$$\begin{gathered}\dot{x}(t) = Ax(t) + (BL)u(t) + \mathfrak{D} \\ \mathfrak{D} = \Delta B u(t) + bf(x) + d\end{gathered} \tag{1}$$

where $x = [x_1 x_2]^T \in R^2$ denotes the system's state vector, $f(x)$ is a nonlinear system function, Δf and Δg are parametric uncertainties, and d represents the external disturbances. L is a post-fault coefficient with $L = diag([l_1, \cdots, l_n)]$, and $l_{i(i=1,\cdots,n)}$, $0 \le l_i \le 1$ represent the level of actuator effectiveness. If $l_i = 1$, the ith actuator acts faultlessly; otherwise, the ith actuator tolerates a certain level of fault with a special case $l_i = 0$, denoting the complete failure of the ith actuator. A and B are matrices with suitable dimensions. Without losing generalities, we assume $x(t) = \left[x_1^T(t)\ x_2^T(t)\right]^T$, $A = \begin{bmatrix} A_{11} & A_{12} \\ A_{21} & A_{22} \end{bmatrix}$, $\Delta B = [0\ \Delta B_2]^T$, and $B = \left[0\ B_2^T\right]^T$, $L = [0\ L_2]^T$.
where B_2 and L_2 are a nonsingular $m \times m$ matrix.

System (1) can be re-written as:

$$\begin{aligned}\dot{x}_1(t) &= A_{11}x_1(t) + A_{12}x_2(t), \\ \dot{x}_2(t) &= A_{21}x_1(t) + A_{22}x_2(t) + (B_2L_2)u(t) + \mathfrak{D}\end{aligned} \tag{2}$$

Assumption 1. *Pair (A, B) is totally controllable. Using this assumption for (2), the controllability of* (A_{11}, A_{12}) *can be obtained by the controllability of (A, B).*

Assumption 2. *The parametric uncertainty and external disturbance term* D_x *is bounded and is less than* η_k*, i.e.,*

$$\|D_x\| < \eta_k \tag{3}$$

Lemma 1. *Schur Complement [36]: for the symmetric matrix* $M = \begin{bmatrix} A & B \\ B^T & D \end{bmatrix}$*, where* $A = A^T$*,* $B = C^T$*, and* $D = D^T$*, the condition M < 0 is equivalent to D < 0 and* $A - BD^{-1}B^T < 0$.

3. Main Results

For system (2), define the switching function as:

$$s(t) = G\left(x(t) - x(0)e^{-\beta t}\right) \tag{4}$$

with:

$$G = \begin{bmatrix} G_1 & I_m \end{bmatrix} \tag{5}$$

where I_m, β, and G_1 are the $m \times m$ identity matrix, the appropriate positive matrix, and $m \times (n - m)$ an appropriate matrix to be designed later, respectively. When $s(t) = 0$ is reached, (3) yields:

$$x_2(\mathrm{t}) = -G_1x_1(\mathrm{t}) + Gx(0)e^{-\beta t} \tag{6}$$

The SMC dynamics are obtained from (2) and (4) as:

$$\dot{x}_1(t) = (A_{11} - A_{12}G_1)x_1(t) + A_{12}Gx(0)e^{-\beta t} \tag{7}$$

According to Assumption 1, the gain matrix G_1 can be found such that the matrix $\Lambda = A_{11} - A_{12}G_1$ holds the expected eigenvalues. Hence, there are two positive constants a and b such that $\|e^{\Lambda t}\| \le ae^{-bt}$. By solving (7), the following formula can be reached:

$$x_1(\mathrm{t}) = e^{\Lambda t}x_1(0) + \int_0^t e^{\Lambda(t-\tau)}A_{12}Gx(0)e^{-\beta t}d\tau \tag{8}$$

where the following inequality for $x_1(t)$ is satisfied:

$$\begin{aligned} &\|x_1(\mathrm{t})\| \le ae^{-bt}\|x_1(0)\| + a\|A_{12}\mathrm{G}\|\|x(0)\|e^{-bt}\int_0^t e^{(b-\beta)}d\tau \\ &= ae^{-bt}\|x_1(0)\| + a\|A_{12}\mathrm{G}\|\|x(0)\|\frac{e^{-\beta t} - e^{-bt}}{b-\beta} \end{aligned} \tag{9}$$

where from (9), the following relation can be reached:

$$\lim_{t\to\infty} x_1(\mathrm{t}) = 0 \tag{10}$$

Thus, the SMC dynamics (7) are asymptotically stable.

Remark 1. *Compared to the sliding surface $s_c(t) = Gx(t)$, to acquire the sliding surface from the beginning, the sliding surface (4) forces the state tracks. As a consequence, the reaching phase is omitted, and the system's invariance to uncertainties and parametric alternation is achieved in the entire system response.*

For the global sliding surface, by using (3) and Remark 1, $s(t) = 0$ implies that:

$$\dot{s}_c(t) = s_c(0)e^{-\beta t} \tag{11}$$

where the first-order differential equation is the special solution. This equation is described as follows:

$$\dot{s}_c(t) - \beta s_c(t) = 0 \tag{12}$$

Then, employing (5) and (10), the global sliding state dynamics are represented as follows:

$$\begin{bmatrix} \dot{x}_1(t) \\ \dot{s}_c(t) \end{bmatrix} = \begin{bmatrix} A_{11} - A_{12}G_1 & A_{12} \\ 0 & -\beta \end{bmatrix} \tag{13}$$

where the characteristic equation of the dynamics (13) can be calculated as follows:

$$(\lambda + \beta)|\lambda I - A_{12} + A_{12}G_1| = 0 \tag{14}$$

where λ is the system's eigenvalue. Hence, the dynamic system's eigenvalues can be positioned in the expected places by suitably developing the parameters β and G_1. The LMI technique is employed to obtain the G_1 interest matrix in the following theorem.

Theorem 1. *By assuming the dynamic system (7), if matrices X > 0, Y and W > 0 are of suitable dimensions, the following LMI must be met:*

$$\begin{bmatrix} A_{11}X - A_{11}Y + XA_{11}^T - Y^TA_{12}^T & X \\ X & -W \end{bmatrix} < 0 \tag{15}$$

then, using $P = X^{-1}$ and $G_1 = YX^{-1}$ in (4), system (7) is asymptotically steady.

Proof. The Lyapunov function is suggested as:

$$v_1 = x_1^T(\mathrm{t})\mathrm{P}x_1(\mathrm{t}) \tag{16}$$

where P is a positive symmetric definite matrix. The differentiation of the Lyapunov function must be obtained along the trajectories of system (7):

$$\begin{aligned}\dot{v}_1(x_1) &= x_1^T(\mathrm{t})\mathrm{P}\dot{x}_1(\mathrm{t}) + \dot{x}_1^T(\mathrm{t})\mathrm{P}x_1(\mathrm{t}) \\ &= x_1^T(\mathrm{t})\{P(A_{11} - A_{12}G_1) + (A_{11} - A_{12}G_1)^T P\}x_1(\mathrm{t}) \\ &+ x_1^T(\mathrm{t})PA_{12}Gx(0)e^{-\beta t} + \left(A_{12}Gx(0)e^{-\beta t}\right)^T Px_1(\mathrm{t})\end{aligned} \tag{17}$$

Considering $\lim\limits_{t\to\infty} e^{-\beta t} = 0$ and assuming that the following inequality is satisfied:

$$P(A_{11} - A_{12}G_1) + (A_{11} - A_{12}G_1)^T P \leq -W^{-1} \tag{18}$$

Then, Equation (17) can be simplified as follows:

$$\dot{v}_1(x_1) \leq -x_1^T(\mathrm{t})W^{-1}x_1(\mathrm{t}) \leq -\lambda_{min}\left(W^{-1}\right)\|x_1(\mathrm{t})\|^2 \tag{19}$$

where $\lambda_{min}(0)$ represents the minimum eigenvalue W^{-1}.

It can easily be shown that a sufficient condition for (17) is:

$$\dot{v}_1(x_1) \leq -\alpha_1 v_1(x_1) \tag{20}$$

where

$$\alpha_1 = \frac{\lambda_{min}(W^{-1})}{\lambda_{max}(P)} \tag{21}$$

Since W > 0 and P > 0, it is clear that the parameter α_1 is scalar positive. Assuming $X = P^{-1}$, and before and after multiplying by X in (18) offers the following results:

$$A_{11}X - A_{12}G_1X + XA_{11}^T - XG_1^TA_{12}^T \leq -XW^{-1}X \tag{22}$$

By defining $Y = G_1X$ and using the Schur supplement in (22), it can be observed that LMI (15) is inferred. Thus, if LMI (15) is possible, the sliding state dynamics (7) are asymptotically stable. □

Differentiating $x_2(t)$ in (4) results in:

$$\dot{x}_2(t) = -G_1(A_{11}x_1(\mathrm{t}) + A_{12}x_2(\mathrm{t})) - \beta Gx(0)e^{-\beta t} \tag{23}$$

If the right-hand side (2) and (23) are equal, the following equivalent control law will be obtained:

$$\begin{aligned}u_{eq}(t) = -(B_2L_2)^{-1}[&(A_{21} + G_1A_{11})x_1(\mathrm{t}) + (A_{22} + G_1A_{12})x_2(\mathrm{t}) + \beta s_c(t)e^{-\beta t} \\ &+ B_2L_2f(x)],\end{aligned} \tag{24}$$

Theorem 2. *Assume the indeterminate nonlinear system (2) and the equivalent control law (24). Suppose that the gain matrix G_1 is acquired from Theorem 1. Using the control rule:*

$$u(t) = u_{eq}(t) + u_N(t) \tag{25}$$

with

$$u_N(t) = -(B_2L_2)^{-1}\hat{Q}sgn(s), \tag{26}$$

An adaptive controller based on the barrier operation is suggested. Utilizing the proposed barrier-based ASMC technique, the external disturbance can be approximated more effectively, and the closed-loop system can evolve steadier. Using the barrier function, the switching control law can be developed in (26) as follows [37,38]:

$$\hat{Q}(t) = \begin{cases} Q_a & if\ 0 < t < \bar{t} \\ Q_{psb} & if\ t > \bar{t} \end{cases} \tag{27}$$

where $\bar{t}$ is the time that the state trajectories converge to the vicinity of the FTSM surface s. The adaptive-tuning rule and the positive-semi-definite barrier function are given by:

$$\begin{cases} \dot{Q}_a = \rho\|s\| \\ Q_{psb} = \frac{\|s\|}{\varepsilon - \|s\|} \end{cases} \tag{28}$$

where $\varepsilon, \rho > 0$. Employing the adaptation rule (26), the control gain $\hat{Q}$ is raised until the state trajectories reach the vicinity ε of the fast terminal sliding surface s at time $\bar{t}$. Then, for the times after $\bar{t}$, the adaptive control gain $\hat{Q}$ switches to the positive-semi-definite barrier function, which can decrease the convergence region and maintain the system states within. In what follows, the stability of the system is verified in two conditions: (a) $0 < t < \bar{t}$ and (b) $t > \bar{t}$.

Theorem 3. *Consider the disturbed nonlinear system (6). Using the adaptive control law (25) with the equivalent controller (24) and the discontinuous controller (26) considering $\hat{Q}(t) = Q_a$, the system state trajectories reach the neighborhood of the sliding surface in finite time.*

Proof. Define the Lyapunov candidate function as:

$$v_2 = \frac{1}{2}\left(s^T s + \vartheta^{-1}\left(Q_a - Q\right)^2\right) \Rightarrow \dot{v}_2 = s^T\dot{s} + \vartheta^{-1}(Q_a - Q)\dot{Q}_a \tag{29}$$

where $\vartheta > 0$, and Q is a positive unknown constant. The time derivative of $\dot{v}_2$ is:

$$\dot{v}_2 = s^T\dot{s} + \vartheta^{-1}(Q_a - Q)\dot{Q}_a \tag{30}$$

Substituting the time derivative of the switching function into the above equation, we obtain:

$$\dot{v}_2 = s^T\left(G\left(Ax(t) + B_2L_2u(t) + B_2L_2f(x) + D + \beta x(0)e^{-\beta t}\right)\right) + \vartheta^{-1}(Q_a - Q)\rho\|S\| \tag{31}$$

Replacing the adaptive control law (25) in the above equation yields:

$$\begin{aligned} \dot{v}_2 &= -s^T((Q_a)sign(s) - D) + \rho\vartheta^{-1}(Q_a - Q)\|\delta\| \\ &\le \|s\|\|D\| - s^T Q_a sign(s) + \rho\vartheta^{-1}(Q_a - Q)\|\delta\| \\ &\le \|s\|\|D\| - Q_a\|s\| + \rho\vartheta^{-1}(Q_a - Q)\|\delta\| \\ &\le \|s\|\|D\| - Q_a\|s\| + \rho\vartheta^{-1}(Q_a - Q)\|\delta\| + Q\|\delta\| - Q\|\delta\| \\ &\le -(Q - \|D\|)\|s\| - \left(1 - \rho\vartheta^{-1}(Q_a - Q)\right)\|s\| \end{aligned} \tag{32}$$

where $\|D\| < \eta$. Because $Q - \|D\| > 0$ and $\rho\vartheta^{-1} < 1$, Equation (32) is written as:

$$\begin{aligned} \dot{v}_1 &\le -\sqrt{2}(Q - \|D\|)\frac{\|s\|}{\sqrt{2}} - \sqrt{2}\vartheta\left(1 - \rho\vartheta^{-1}\right)\frac{(Q_a - Q)}{\sqrt{2}\vartheta} \\ &\le -min\left\{\sqrt{2}(Q - \|D\|), \sqrt{2}\vartheta\left(1 - \rho\vartheta^{-1}\right)\|\delta\|\right\}\left(\frac{\|s\|}{\sqrt{2}} + \frac{\|Q_a - Q\|}{\sqrt{2}\vartheta}\right) \le -\chi v_2^{\frac{1}{2}} \end{aligned} \tag{33}$$

□

Theorem 4. *For system (2), using the adaptive control law (25) with the equivalent controller (24) and the discontinuous controller (26), taking into consideration* $\hat{Q} = Q_{psb}$ *(Equation (27)), yields:*

$$u = -(B_2L_2)^{-1}[(A_{21} + G_1A_{11})x_1(t) + (A_{22} + G_1A_{12})x_2(t) + \beta s_c(t)e^{-\beta t} + B_2L_2f(x)] - (B_2L_2)^{-1}Q_{psb}sgn(s), \tag{34}$$

Then, the state of the system reaches the convergence region $\|\delta\| < \varepsilon$ *in finite time.*

Proof. Define the Lyapunov function as:

$$v_3 = \frac{1}{2}(s^Ts + \Big(Q_{psb} - Q_{psb}(0))^2\Big) \tag{35}$$

Differentiating the Lyapunov function (35) with respect to time yields:

$$\dot{v}_3 = s^T\dot{s} + \Big(Q_{psb} - Q_{psb}(0)\Big)\dot{Q}_{psb} \tag{36}$$

Substituting $\dot{s}$ and $Q_{psb}(0) = 0$ into the above equation, we obtain:

$$\dot{v}_3 = s^T\Big(G\Big(Ax(t) + B_2L_2u(t) + B_2L_2f(x) + D + \beta x(0)e^{-\beta t}\Big)\Big) + Q_{psb}\dot{Q}_{psb} \tag{37}$$

Substituting the control law (25) into (37) gives:

$$\begin{aligned}
\dot{v}_3 &= -s^T\Big(Q_{psb}sign(s) - D\Big) + Q_{psb}\dot{Q}_{psb} \le \|s\|\|D\| - Q_{psb}\|s\| + Q_{psb}\dot{Q}_{psb} \\
&\le -\Big(Q_{psb} - \|D_x\|\Big)\|s\| + Q_{psb}(\tfrac{\varepsilon}{(\varepsilon - \|s\|)^2})sign(s)\dot{s} \\
&\le -\mu\|s\| - \Big(Q_{psb} - \|D_x\|\Big)\|s\| \\
&\le -\Big(Q_{psb} - \|D\|\Big)\|s\| + Q_{psb}(\tfrac{\varepsilon}{(\varepsilon - \|s\|)^2})sign(s)\dot{s} \\
&\le -\Big(Q_{psb} - \|D\|\Big)\|s\| \\
&\quad -Q_{psb}(\tfrac{\varepsilon}{(\varepsilon - \|s\|)^2})sign(s)\Big(\Big(Q_{psb}\Big)sign(s) - D\Big) \\
&\le -\Big(Q_{psb} - \|D\|\Big)\|s\| - \tfrac{\varepsilon}{(\varepsilon - \|s\|)^2}\Big(Q_{psb} - \|D\|\Big)\|s\|Q_{psb}
\end{aligned} \tag{38}$$

where because $Q_{psb} > \|D_x\|$ and $\frac{\varepsilon}{(\varepsilon - \|s\|)^2} > 0$, one finds:

$$\begin{aligned}
\dot{v}_3 &\le -\sqrt{2}\Big(Q_{psb} - \|D\|\Big)\tfrac{\|s\|}{\sqrt{2}} - \tfrac{\sqrt{2}\varepsilon}{(\varepsilon - \|s\|)^2}\Big(Q_{psb} - \|D\|\Big)\tfrac{\|s\|Q_{psb}}{\sqrt{2}}, \\
&\le -\sqrt{2}\Big(Q_{psb} - \|D\|\Big)min\Big\{1, \tfrac{\varepsilon}{(\varepsilon - \|D\|)^2}\Big\}(\tfrac{\|s\|}{\sqrt{2}} + \tfrac{\|s\|Q_{psb}}{\sqrt{2}}) \le -\Omega v_3{}^{\frac{1}{2}}
\end{aligned} \tag{39}$$

where $\Omega = \sqrt{2}\Big(Q_{psb} - \|D\|\Big)min\Big\{1, \frac{\varepsilon}{(\varepsilon - \|D\|)^2}\Big\}$. □

Unwanted responses can occur in the control system due to the discontinuous nature of the sign function provided in controls (26). Therefore, the sign(.) function is substituted by the continuous hyperbolic tangent function to modify the slope of the tanh(.) function. In other words, the hyperbolic tangent function is used as an approximation of the discontinuous sign function. The chattering phenomenon is avoided by decreasing the steepness of the tanh(.) function. Using the continuous hyperbolic tangent function in the control law (25) yields:

$$u_N(t) = -(B_2L_2)^{-1}\hat{Q}\tanh(s(t)/\zeta), \tag{40}$$

where $sgn(s(t)/\zeta) \approx \tanh(s(t)/\zeta)$ and ζ is the thickness coefficient of the boundary layer.

Substituting Equations (24) and (26) in (25) yields the following control law:

$$u = -(B_2L_2)^{-1}[(A_{21} + G_1A_{11})x_1(\mathrm{t}) + (A_{22} + G_1A_{12})x_2(\mathrm{t}) + \beta s_c(t)e^{-\beta t} \\ +B_2L_2f(x)] - (B_2L_2)^{-1}\hat{Q}\tanh(s(t)/\zeta) \tag{41}$$

Theorem 5. *In the following proof, this time, $\hat{Q}(t) = Q_a$ is considered. In this part, as in the previous theorem, the sign(.) function is replaced by the tanh(.) function.*

Proof. Define the Lyapunov candidate function as:

$$v_2 = \frac{1}{2}(s^Ts + \vartheta^{-1}\left(Q_a - Q\right)^2\right) \Rightarrow \dot{v}_2 = s^T\dot{s} + \vartheta^{-1}(Q_a - Q)\dot{Q}_a$$

where $\vartheta > 0$, and Q is a positive unknown constant.

The time derivative of $\dot{v}_2$ is given by:

$$\dot{v}_2 = s^T\dot{s} + \vartheta^{-1}(Q_a - Q)\dot{Q}_a$$

Substituting (3) into the above equation yields:

$$\dot{v}_2 = s^T(G\left(Ax(t) + B_2L_2u(t) + B_2L_2f(x) + D + \beta x(0)e^{-\beta t}\right) + \vartheta^{-1}(Q_a - Q)\rho\|S\|,$$

Substituting the adaptive control law in the above equation yields:

$$\begin{aligned}\dot{v}_2 &= -s^T((Q_a)\tanh(s(t)/\zeta) - D) + \rho\vartheta^{-1}(Q_a - Q)\|s\| \\ &\leq \|s\|\|D\| - s^TQ_a\tanh(s(t)/\zeta) + \rho\vartheta^{-1}(Q_a - Q)\|s\|\end{aligned} \tag{42}$$

The following equation is obtained:

$$-(Q_a)\tanh(\frac{s}{\zeta}) \leq 0 \tag{43}$$

□

Assumption 3. *For the non-zero and positive values of σ_1 and σ_2, the following relation is established*:

$$\sigma_1 \leq 1 \leq \sigma_2 \tag{44}$$

Considering Assumption 3 and multiplying Equation (44) by u^2 yields:

$$\sigma_1u^2 \leq u^2 \leq \sigma_2u^2 \tag{45}$$

From Equations (45) and (43), the following condition is obtained as:

$$\begin{aligned}&\sigma_1\left[\tfrac{1}{\sigma_1^2}(Q_a)^2(\tanh(\tfrac{s}{\zeta}))^2\right] \leq u(t) \times u(t) \\ &= -\tfrac{1}{\sigma_1}(Q_a)\tanh(\tfrac{s}{\zeta})u(t)\end{aligned} \tag{46}$$

Multiplying both sides of the above equation by $(\frac{s}{\zeta})^2 > 0$ simplifies it to:

$$\frac{s}{\zeta}u(t) \leq -(Q_a)\|\frac{s}{\zeta}\| \tag{47}$$

Combining Equations (42) and (47) yields:

$$\begin{aligned} \dot{v}_2 &\leq \|s\|\|D\| - Q_a\|s\| + \rho\vartheta^{-1}(Q_a - Q)\|\delta\| \\ &\leq \|s\|\|D\| - Q_a\|s\| + \rho\vartheta^{-1}(Q_a - Q)\|\delta\| + Q\|\delta\| - Q\|\delta\| \\ &\leq -(Q - \|D\|)\|s\| - \left(1 - \rho\vartheta^{-1}(Q_a - Q)\right)\|s\| \end{aligned} \tag{48}$$

where $\|D\| < \eta$. Because $Q - \|D\| > 0$ and $\rho\vartheta^{-1} < 1$, Equation (32) is written as:

$$\begin{aligned} \dot{v}_2 &\leq -\sqrt{2}(Q - \|D\|)\tfrac{\|s\|}{\sqrt{2}} - \sqrt{2}\vartheta(1 - \rho\vartheta^{-1})\tfrac{(Q_a - Q)}{\sqrt{2}\vartheta} \\ &\leq -min\left\{\sqrt{2}(Q - \|D\|), \sqrt{2}\vartheta(1 - \rho\vartheta^{-1})\|\delta\|\right\}\left(\tfrac{\|s\|}{\sqrt{2}} + \tfrac{\|Q_a - Q\|}{\sqrt{2}\vartheta}\right) \leq -\chi v_2^{\frac{1}{2}} \end{aligned} \tag{49}$$

Theorem 6. *In the following proof, we consider $\hat{Q}(t) = Q_{psb}$. In this part, as in the previous theorem, the sign(.) function is replaced by the tanh(.) function.*

Proof. Consider the same Lyapunov function as that in (35):

$$v_3 = \frac{1}{2}(s^T s + \left(Q_{psb} - Q_{psb}(0)\right)^2\Big),$$

Now, differentiating the Lyapunov function with respect to time, we have:

$$\dot{v}_3 = s^T\dot{s} + \left(Q_{psb} - Q_{psb}(0)\right)\dot{Q}_{psb}$$

Substituting $\dot{s}$ and $Q_{psb}(0) = 0$ into the above equation, we obtain:

$$\dot{v}_3 = s^T(G\left(Ax(t) + B_2L_2u(t) + B_2L_2f(x) + D + \beta x(0)e^{-\beta t}\right) + Q_{psb}\dot{Q}_{psb}$$

Substituting the control law (22) into (35) yields:

$$\begin{aligned} \dot{v}_3 &= -s^T\left(Q_{psb}\tanh(s(t)/\zeta) - D\right) + Q_{psb}\dot{Q}_{psb} \\ &\leq \|s\|\|D\| - Q_{psb}\|s\| + Q_{psb}\dot{Q}_{psb} \\ &\leq -\left(Q_{psb} - \|D_x\|\right)\|s\| + Q_{psb}\left(\tfrac{\varepsilon}{(\varepsilon - \|s\|)^2}\right)\tanh(s(t)/\zeta)\dot{s} \\ &\leq -\mu\|s\| - \left(Q_{psb} - \|D_x\|\right)\|s\| \\ &\leq -\left(Q_{psb} - \|D\|\right)\|s\| + Q_{psb}\left(\tfrac{\varepsilon}{(\varepsilon - \|s\|)^2}\right)\tanh(s(t)/\zeta)\dot{s} \\ &\leq -\left(Q_{psb} - \|D\|\right)\|s\| - Q_{psb}\left(\tfrac{\varepsilon}{(\varepsilon - \|s\|)^2}\right)\tanh(s(t)/\zeta)\left(\left(Q_{psb}\right)\tan h(s(t)/\zeta) - D\right) \end{aligned} \tag{50}$$

Consider Assumption 2, and multiplying u^2 to Equation (50), we have

$$\dot{v}_3 \leq -\left(Q_{psb} - \|D\|\right)\|s\| - \frac{\varepsilon}{(\varepsilon - \|s\|)^2}\left(Q_{psb} - \|D\|\right)\|s\|Q_{psb}$$

where because $Q_{psb} > \|D_x\|$ and $\frac{\varepsilon}{(\varepsilon - \|s\|)^2} > 0$, one finds:

$$\begin{aligned} \dot{v}_3 &\leq -\sqrt{2}\left(Q_{psb} - \|D\|\right)\tfrac{\|s\|}{\sqrt{2}} - \tfrac{\sqrt{2}\varepsilon}{(\varepsilon - \|s\|)^2}\left(Q_{psb} - \|D\|\right)\tfrac{\|s\|Q_{psb}}{\sqrt{2}}, \\ &\leq -\sqrt{2}\left(Q_{psb} - \|D\|\right)min\left\{1, \tfrac{\varepsilon}{(\varepsilon - \|D\|)^2}\right\}\left(\tfrac{\|s\|}{\sqrt{2}} + \tfrac{\|s\|Q_{psb}}{\sqrt{2}}\right) \leq -\Omega v_3^{\frac{1}{2}} \end{aligned} \tag{51}$$

where $\Omega = \sqrt{2}\left(Q_{psb} - \|D\|\right)min\left\{1, \frac{\varepsilon}{(\varepsilon - \|D\|)^2}\right\}$. □

4. Simulation Results

To assess the performance of the proposed approach, we consider the following Genesio's chaotic system with parametric uncertainty, external disturbance, and actuator fault:

$$\begin{bmatrix} \dot{x}_1(t) \\ \dot{x}_2(t) \\ \dot{x}_3(t) \end{bmatrix} = \begin{bmatrix} 0 & 1 & 0 \\ 0 & 0 & 1 \\ -6 & -2.92 & -1.2 \end{bmatrix} \begin{bmatrix} x_1(t) \\ x_2(t) \\ x_3(t) \end{bmatrix} + \left(\begin{bmatrix} 0 \\ 0 \\ 1 \end{bmatrix} \times L_2 + \begin{bmatrix} 0 \\ 0 \\ -0.1\sin(t) \end{bmatrix} \right) u(t) + \begin{bmatrix} 0 \\ 0 \\ x_1^2(t) \end{bmatrix} + \begin{bmatrix} 0.001\sin(0.005t) \\ 0.005\cos(0.001t) \\ 0.009\sin(0.001t) \end{bmatrix} \tag{52}$$

where expressing it as Equation (2) gives:

$$A_{11} = [0],\ A_{12} = [1\ 0],\ A_{21} = \begin{bmatrix} 0 \\ -6 \end{bmatrix},\ A_{22} = \begin{bmatrix} 0 & 1 \\ -2.92 & -1.2 \end{bmatrix},\ B_2 = \begin{bmatrix} 1 & 0 \\ 0 & 1 \end{bmatrix},$$

The parametric uncertainty and nonlinear function are considered as follows:

$$\Delta B_2 = -0.1\sin(t),\ f(x) = \begin{bmatrix} 0 \\ 0 \\ x_1^2(t) \end{bmatrix}$$

where L_2 is the fault coefficient entered into the system input. The type of this fault is sinusoidal, and its magnitude is 50%. This fault is applied to the system inputs at the 20th second.

For simulation purposes, we consider $\beta = 3$. Matrices P, Y, W, and G_1 are obtained using the MATLAB LMI toolbox as follows:

$$P = [13.3333],\ Y = \begin{bmatrix} 2.2066 \\ 0 \end{bmatrix},\ W = [4.8044],\ G_1 = [29.4210; 0].$$

If the initial conditions are selected as follows:

$$x_0(t) = [1 - 2\ \ 5]^T, \tag{53}$$

The simulation results are depicted in Figures 1–3. Figure 1 shows the dynamics of the sliding surfaces resulting from both controllers. Note the chattering behavior exhibited by the sliding surface of the ASMC method even before the application of the fault. A sharp increase in chattering was noticed following the fault application. In contrast, with the help of the barrier function and hyperbolic tangent, the proposed controller was able to reduce the amount of chattering both before and after fault occurrence.

Figure 2 displays the control effort for both approaches. As can be seen, chattering is noticeable using the ASMC method, both before and after fault occurrence. It was intensified after fault occurrence. The proposed approach, on the other hand, was able to eliminate this phenomenon to a large extent.

Figure 3 shows the system state outputs. In all three states depicted in Figure 3, it is clear that regardless of the external disturbances, actuator fault, and parametric uncertainty, the proposed controller yields the least chattering and tracking errors. The ASMC controller proposed in [35] was unable to eliminate this phenomenon, both pre- and post-fault, with chattering sharply intensifying following fault occurrence.

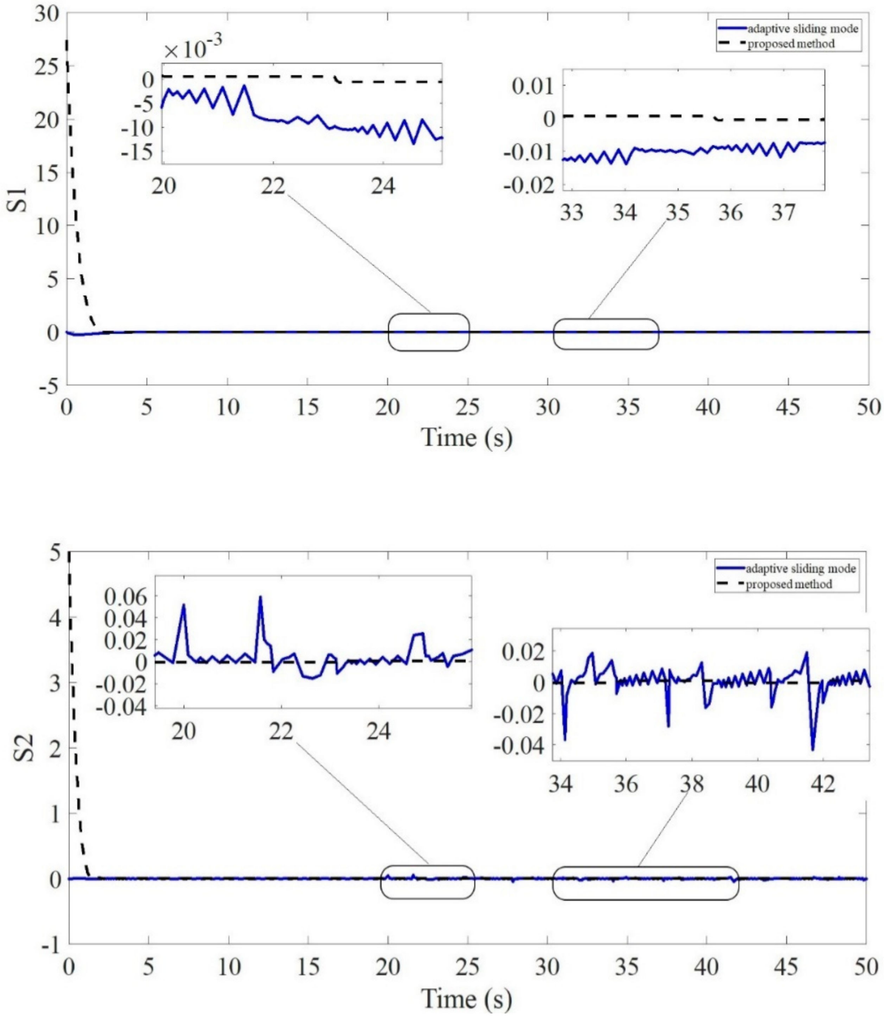

Figure 1. The system's sliding surfaces in the presence of 50% sinusoidal fault.

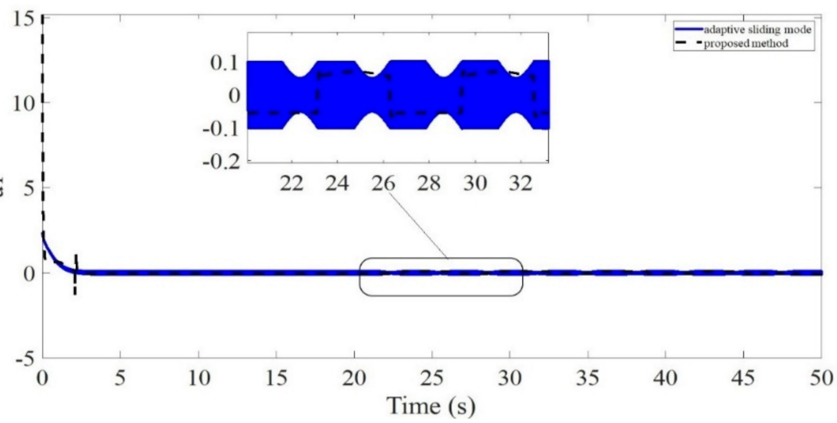

Figure 2. *Cont*.

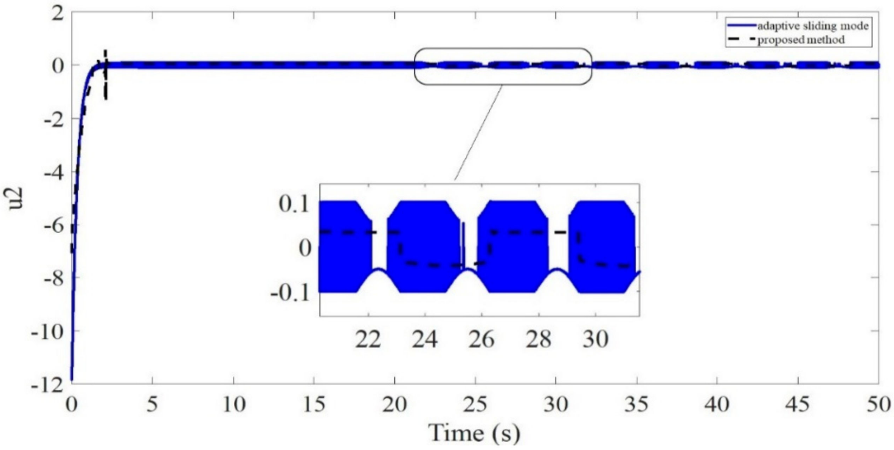

Figure 2. The control input under 50% sinusoidal fault.

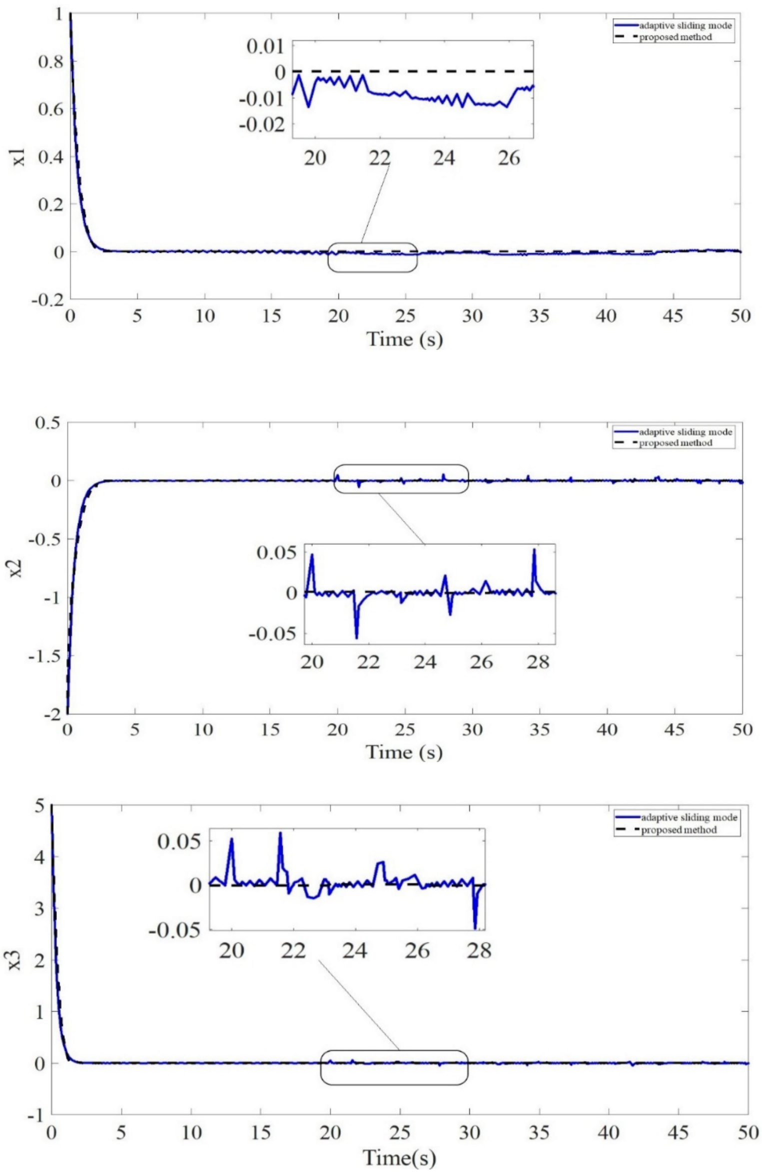

Figure 3. System states under 50% sinusoidal fault.

5. Conclusions and Future Work

This paper proposes an adaptive barrier GSMC approach based on LMIs and hyperbolic tangent functions to mitigate the effects of external disturbances, parametric uncertainties, and actuator faults. The main attributes of the proposed approach are as follows: (1) GSMC based on LMI is used to find the optimal coefficients of the sliding surface. (2) An adaptive barrier function is used to ensure the convergence of the output variables independent of the high gain of the disturbances and to avoid overshooting. (3) The traditional sign function is replaced by a hyperbolic tangent function to reduce the chattering effects resulting from external disturbances and actuator faults. Validation of the proposed approach using the Genesio's chaotic system, subject to parametric uncertainties and external disturbances, and comparison analysis with an ASMC approach confirm its superior dynamics and tracking performance. We suggest that future work combine higher order global sliding modes with MPC, a barrier function, and a hyperbolic tangent to mitigate actuator faults for underactuated systems.

Author Contributions: Conceptualization, K.N., M.T.V. and S.M.; formal analysis, S.M., A.F., A.N. and M.T.V.; funding acquisition, A.F.; investigation, S.M., A.F., K.N. and M.T.V.; methodology, A.N. and S.M.; writing—original draft, K.N., M.T.V. and A.N.; writing—review and editing, and supervision, S.M., A.F., A.N. and M.T.V. All authors have read and agreed to the published version of the manuscript.

Funding: This research received no external funding.

Institutional Review Board Statement: Not applicable.

Informed Consent Statement: Not applicable.

Data Availability Statement: The data that support the findings of this study are available within the article.

Conflicts of Interest: The authors declare no conflict of interest.

References

1. Jankowska, K.; Dybkowski, M. A Current Sensor Fault Tolerant Control Strategy for PMSM Drive Systems Based on Cri Markers. *Energies* **2021**, *14*, 3443. [CrossRef]
2. Nguyen, N.P.; Mung, N.X.; Thanh Ha, L.N.N.; Huynh, T.T.; Hong, S.K. Finite-time attitude fault tolerant control of quadcopter system via neural networks. *Mathematics* **2020**, *8*, 1541. [CrossRef]
3. Ducard, G.J. *Fault-Tolerant Flight Control and Guidance Systems: Practical Methods for Small Unmanned Aerial Vehicles*; Springer Science & Business Media: Berlin/Heidelberg, Germany, 2009.
4. Blanke, M.; Kinnaert, M.; Lunze, J.; Staroswiecki, M.; Schröder, J. *Diagnosis and Fault-Tolerant Control*; Springer: Berlin/Heidelberg, Germany, 2006; Volume 2.
5. Xu, S.; Wang, W.; Chen, S.-Y. Robust Fault-Tolerant Control for Stochastic Port-Hamiltonian Systems against Actuator Faults. *Mathematics* **2022**, *10*, 1477. [CrossRef]
6. Fekih, A.; Mobayen, S.; Chen, C.-C. Adaptive Robust Fault-Tolerant Control Design for Wind Turbines Subject to Pitch Actuator Faults. *Energies* **2021**, *14*, 1791. [CrossRef]
7. Edwards, C.; Lombaerts, T.; Smaili, H. *Fault Tolerant Flight Control*; Lecture Notes in Control and Information Sciences; Springer: Berlin/Heidelberg, Germany, 2010; Volume 399, pp. 1–560.
8. Isermann, R.; Ballé, P. Trends in the application of model based fault detection and diagnosis of technical processes. *IFAC Proc. Vol.* **1996**, *29*, 6325–6336. [CrossRef]
9. Zhang, D.; Wang, Z.; Hu, S. Robust satisfactory fault-tolerant control of uncertain linear discrete-time systems: An LMI approach. *Int. J. Syst. Sci.* **2007**, *38*, 151–165. [CrossRef]
10. Lee, T.H.; Lim, C.P.; Nahavandi, S.; Roberts, R.G. Observer-Based H_∞ Fault-Tolerant Control for Linear Systems with Sensor and Actuator Faults. *IEEE Syst. J.* **2018**, *13*, 1981–1990. [CrossRef]
11. Hamayun, M.T.; Edwards, C.; Alwi, H. Design and analysis of an integral sliding mode fault-tolerant control scheme. *IEEE Trans. Autom. Control* **2011**, *57*, 1783–1789. [CrossRef]
12. Wang, T.; Xie, W.; Zhang, Y. Sliding mode fault tolerant control dealing with modeling uncertainties and actuator faults. *ISA Trans.* **2012**, *51*, 386–392. [CrossRef]
13. Ejaz, F.; Hamayun, M.T.; Hussain, S.; Ijaz, S.; Yang, S.; Shehzad, N.; Rashid, A. An adaptive sliding mode actuator fault tolerant control scheme for octorotor system. *Int. J. Adv. Robot. Syst.* **2019**, *16*, 1729881419832435. [CrossRef]

14. Gao, Z.; Jiang, B.; Shi, P.; Qian, M.; Lin, J. Active fault tolerant control design for reusable launch vehicle using adaptive sliding mode technique. *J. Frankl. Inst.* **2012**, *349*, 1543–1560. [CrossRef]
15. Wang, B.; Zhang, Y. Adaptive sliding mode fault-tolerant control for an unmanned aerial vehicle. *Unmanned Syst.* **2017**, *5*, 209–221. [CrossRef]
16. Zhang, H.; Hu, J.; Yu, X. Adaptive sliding mode fault-tolerant control for a class of uncertain systems with probabilistic random delays. *IEEE Access* **2019**, *7*, 64234–64246. [CrossRef]
17. Kamal, E.; Aitouche, A.; Ghorbani, R.; Bayart, M. Robust fuzzy fault-tolerant control of wind energy conversion systems subject to sensor faults. *IEEE Trans. Sustain. Energy* **2012**, *3*, 231–241. [CrossRef]
18. Zhai, D.; An, L.; Li, J.; Zhang, Q. Adaptive fuzzy fault-tolerant control with guaranteed tracking performance for nonlinear strict-feedback systems. *Fuzzy Sets Syst.* **2016**, *302*, 82–100. [CrossRef]
19. Wang, H.; Wang, Y. Neural-network-based fault-tolerant control of unknown nonlinear systems. *IEE Proc.—Control Theory Appl.* **1999**, *146*, 389–398. [CrossRef]
20. Wang, Z.; Liu, L.; Zhang, H. Neural network-based model-free adaptive fault-tolerant control for discrete-time nonlinear systems with sensor fault. *IEEE Trans. Syst. Man Cybern. Syst.* **2017**, *47*, 2351–2362. [CrossRef]
21. Kiselev, A.; Catuogno, G.R.; Kuznietsov, A.; Leidhold, R. Finite-control-set MPC for open-phase fault-tolerant control of PM synchronous motor drives. *IEEE Trans. Ind. Electron.* **2019**, *67*, 4444–4452. [CrossRef]
22. Morato, M.M.; Sename, O.; Dugard, L. LPV-MPC fault tolerant control of automotive suspension dampers. *IFAC-Pap.* **2018**, *51*, 31–36. [CrossRef]
23. Azizi, A.; Nourisola, H.; Shoja-Majidabad, S. Fault tolerant control of wind turbines with an adaptive output feedback sliding mode controller. *Renew. Energy* **2019**, *135*, 55–65. [CrossRef]
24. Chen, L.; Edwards, C.; Alwi, H.; Sato, M. Flight evaluation of a sliding mode online control allocation scheme for fault tolerant control. *Automatica* **2020**, *114*, 108829. [CrossRef]
25. Van, M. An enhanced robust fault tolerant control based on an adaptive fuzzy PID-nonsingular fast terminal sliding mode control for uncertain nonlinear systems. *IEEE/ASME Trans. Mechatron.* **2018**, *23*, 1362–1371. [CrossRef]
26. Van, M.; Do, X.P.; Mavrovouniotis, M. Self-tuning fuzzy PID-nonsingular fast terminal sliding mode control for robust fault tolerant control of robot manipulators. *ISA Trans.* **2020**, *96*, 60–68. [CrossRef] [PubMed]
27. Van, M.; Mavrovouniotis, M.; Ge, S.S. An adaptive backstepping nonsingular fast terminal sliding mode control for robust fault tolerant control of robot manipulators. *IEEE Trans. Syst. Man Cybern. Syst.* **2018**, *49*, 1448–1458. [CrossRef]
28. Zhao, Y.; Wang, J.; Yan, F.; Shen, Y. Adaptive sliding mode fault-tolerant control for type-2 fuzzy systems with distributed delays. *Inf. Sci.* **2019**, *473*, 227–238. [CrossRef]
29. Pan, Y.; Yang, C.; Pan, L.; Yu, H. Integral sliding mode control: Performance, modification, and improvement. *IEEE Trans. Ind. Inform.* **2017**, *14*, 3087–3096. [CrossRef]
30. Chu, V.K.; Tomizuka, M. Sliding mode control with nonlinear sliding surfaces. *IFAC Proc. Vol.* **1996**, *29*, 2877–2882. [CrossRef]
31. Mehrad, R.; Kargar, S.M. Integrated model predictive fault-tolerant control, and fault detection based on the parity space approach for a reverse osmosis desalination unit. *Trans. Inst. Meas. Control* **2020**, *42*, 1882–1894. [CrossRef]
32. Tang, P.; Lin, D.; Zheng, D.; Fan, S.; Ye, J. Observer based finite-time fault tolerant quadrotor attitude control with actuator faults. *Aerosp. Sci. Technol.* **2020**, *104*, 105968. [CrossRef]
33. Wang, J.; Zhao, Z.; Zheng, Y. NFTSM-based Fault Tolerant Control for Quadrotor Unmanned Aerial Vehicle with Finite-Time Convergence. *IFAC-Pap.* **2018**, *51*, 441–446. [CrossRef]
34. Yang, H.; Yin, S.; Kaynak, O. Neural network-based adaptive fault-tolerant control for Markovian jump systems with nonlinearity and actuator faults. *IEEE Trans. Syst. Man Cybern. Syst.* **2020**, *51*, 3687–3698. [CrossRef]
35. Liu, G.; Wang, S.; Zhang, D.; Shen, Y.; Yao, Z. Fault Tolerant Control Allocation Based on Adaptive Sliding Mode Control for Distributed-Driven Electric Vehicle. In Proceedings of the Chinese Intelligent Automation Conference, Jiangsu, China, 20–22 September 2019; Springer: Berlin/Heidelberg, Germany, 2020; pp. 251–261.
36. Mobayen, S. Design of LMI-based global sliding mode controller for uncertain nonlinear systems with application to Genesio's chaotic system. *Complexity* **2015**, *21*, 94–98. [CrossRef]
37. Obeid, H.; Fridman, L.M.; Laghrouche, S.; Harmouche, M. Barrier function-based adaptive sliding mode control. *Automatica* **2018**, *93*, 540–544. [CrossRef]
38. Laghrouche, S.; Harmouche, M.; Chitour, Y.; Obeid, H.; Fridman, L.M. Barrier function-based adaptive higher order sliding mode controllers. *Automatica* **2021**, *123*, 109355. [CrossRef]